Applications of Time-Domain Metrology to the Automation of Broad-Band Microwave Measurements

A. MURRAY NICOLSON, MEMBER, IEEE, C. LEONARD BENNETT, JR., MEMBER, IEEE, DAVID LAMENSDORF, MEMBER, IEEE, AND LEON SUSMAN, MEMBER, IEEE

Abstract—**It is only recently that measurement of the transient response of microwave systems directly in the time domain has become practicable. It has led to growing interest in the concept of specifying broad-band performance solely by a transient-response measurement. Results of the use of time-domain techniques to obtain, within the range 0.1 to 10 GHz, such data as the S parameters of networks, the constitutive parameters of microwave materials, the driving-point impedance and transfer function of microwave antennas, and the frequency-domain scattering parameters of conducting surfaces in free space are described.**

I. Introduction

IT IS ONLY recently that measurement of the transient response of microwave systems directly in the time domain has become practicable. It has led to growing interest in the concept of specifying broad-band performance solely by a transient-response measurement, but applications do not exist only in the time domain. Since the subnanosecond rise-time responses of broad-band networks contain broad spectral information concerning the networks, through the application of Fourier transforms, many conventional parameters of systems are available in the frequency domain [1]–[3]. This paper describes results of the use of time-domain techniques to obtain, within the range 0.1 to 10 GHz, such data as the S parameters of networks, the constitutive parameters of microwave materials, the driving-point impedance and transfer function of microwave antennas, and the frequency-domain scattering parameters of conducting surfaces in free space. Initially, an automated time-domain measurement system is described in detail. Then the wide variety of applications to which frequency-domain techniques using this system have been applied are discussed.

II. General Principles of Automated Time-Domain Measurements

The three basic elements of the measurement system are a subnanosecond rise-time pulse generator, a broad-band sampling oscilloscope, and an instrumentation computer. Their arrangement for use in a scattering measurement is shown in Fig. 1. The sampling oscilloscope acts essentially as an analog sample-and-hold circuit with an exceptionally narrow sample time (typically 30 ps), allowing a transient response with microwave frequency components to be examined point by point. The generated pulse interacts with the system under test (in this case a scattering surface), and the resultant transient response is sampled at fixed points in time by the sampling oscilloscope. The time position to be sampled is determined by a digital number set up in the computer and output-to-storage register R_1 and a digital-analog converter. The purpose of R_2 will be explained later. The sampled-and-held voltage at the specified time position is smoothed in an averaging circuit, and then digitized for input to the computer, which may operate either in a simple open-loop scanning system or, for high-stability measurements, in a closed-loop error-compensating scheme.

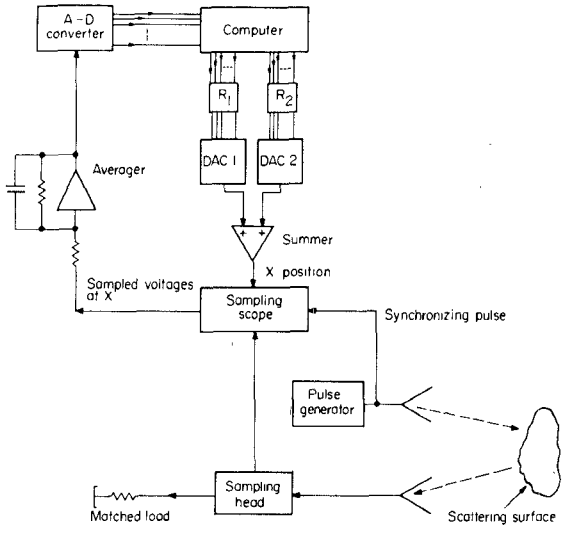

Fig. 1. Time-domain measurement system.

The basic configurations used in microwave measurements which have been made using the system are shown in Fig. 2. In Fig. 2(a) free-space scattering measurements are made using two antennas, the returned transient response from the scatterer being sampled and digitized for input to the computer. Using a feedthrough sampling system, reflection measurements may also be made as shown in Fig. 2(b); this technique is primarily used in closed transmission-line measurements. Free-space measurements, as in Fig. 2(b), are

Manuscript received May 5, 1971; revised September 10, 1971. Portions of this work were supported under U. S. Air Force Contracts F33615-70-C-1722, F30602-69-C-0357, and F30602-70-C-0088.

A. M. Nicolson was with Sperry Rand Research Center, Sudbury, Mass. He is now with the Royal Radar Establishment, Great Malvern, England.

C. L. Bennett, Jr., D. Lamensdorf, and L. Susman are with Sperry Rand Research Center, Sudbury, Mass. 01776.

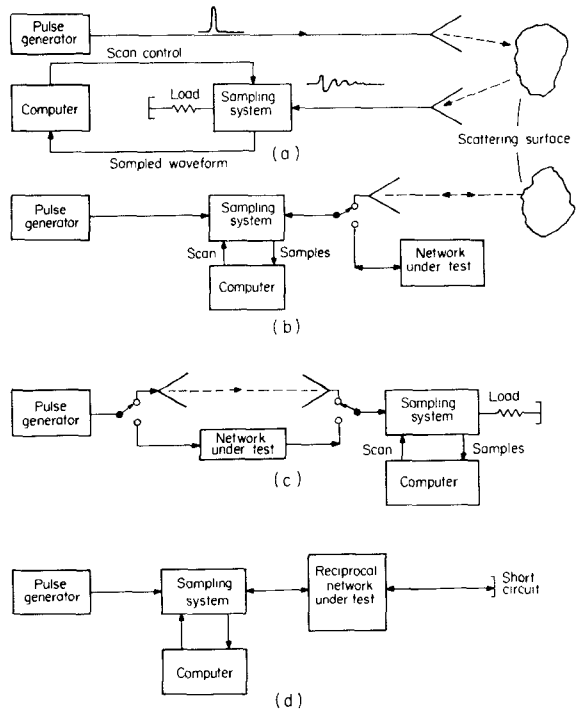

Fig. 2. Basic measurement configurations. (a) and (b) Reflection measurements. (c) and (d) Transmission measurements.

usually impracticable, since in order to obtain a reasonable amplitude of returned signal from a scatterer the generated pulse must be several hundred volts in amplitude, and the sampling system is destroyed by voltages in excess of a few volts. Devices such as directional couplers and circulators have limited capabilities for time-domain work. For transmission measurements in free space or closed lines, the arrangement shown in Fig. 2(c) has been used, while for some reciprocal transmission-line networks the arrangement in Fig. 2(d) may be used; if the network has a short-lived reflection transient response, then measurement over a subsequent later time window will also give the response of the transmitted wave which has traversed the network twice. In fact, the system of Fig. 2(d) can thus yield both reflection and transmission data, and has been applied to microwave materials measurements and to networks with relatively low one-way insertion loss.

The waveform $f_0(nT)$ acquired by the computer comprises N equispaced samples of the response, where N may lie between 64 and 1024. When the equivalent time interval between samples is T, this permits performing the discrete Fourier transform of the response,

$$F_0(k\omega_0) = T \sum_{n=0}^{N-1} f_0(nT) \exp(-jnk\omega_0 T).$$

In the particular case where $\omega_0 = 2\pi/NT$, then

$$F_0(k\omega_0) = T \sum_{n=0}^{N-1} f_0(nT) \exp(-j2\pi nk/N)$$

and when N is "highly composite," and in particular a power of 2, fast Fourier transforms can be used [4]. A similar transform of the waveform of the generated pulse $f_i(nT)$ yields, by taking the ratio of corresponding frequency-domain ordinates, the values of the reflection or transmission coefficients at intervals of ω_0. The sampling interval T must be chosen sufficiently small to sample adequately the highest frequency present in the response, and the time-window width NT must be sufficiently large to encompass all significant portions of the response; these potential sources of error are the aliasing and truncation errors, respectively. It is difficult to predict these errors without full *a priori* knowledge of the waveform being measured, and in practice it proves adequate merely to ensure visually that the most rapidly changing segments of a waveform are sampled at several points and that the time window is wide enough. Inspection of the spectrum around the Nyquist frequency will reveal if sufficient amplitude exists here to cause aliasing errors, and extending the window width will change the spectrum if truncation errors are significant.

Pulse generators useful in time-domain metrology employ mercury switches, tunnel diodes, avalanche transistors, step-recovery diodes, or high-pressure spark gaps. The mercury switch is mounted as a series switch in a coaxial line, abruptly connecting a charged line to the output line and generating a pulse whose length is determined by the charge linelength. With careful design, rise times of less than 100 ps can be achieved [5]. Limited to a repetition rate of 200–300 Hz by mechanical considerations, mercury switches have been applied mainly in free-space applications. The low repetition rate makes some of the complex scanning methods to be described difficult to implement. The tunnel-diode pulser has the fastest rise time available, but its low amplitude limits the maximum measurable insertion loss of components and networks. Many transistors can create subnanosecond rise time pulses when they are driven into avalanche breakdown, and they may be used just as the mercury switch is used to discharge charged transmission lines. The waveform generated, however, is more complex, generally consisting of a fast transition followed by a "roundoff" at the top of the pulse, making definition of rise time difficult. A combination of an avalanche transistor with one or more step-recovery diodes allows generation of pulses with rise times less than 100 ps amplitudes of several volts, and repetition rates up to 1 MHz. Fig. 3 shows the pulse-amplitude spectrum of one such generator compared with that of a tunnel-diode pulse generator, and the improved spectral intensity is apparent. Also shown is the typical spectral noise level.

The spectra of Fig. 3 give the typical signal–noise ratios achievable when the averager of Fig. 1 has a time constant of 30 ms and points are read every 100

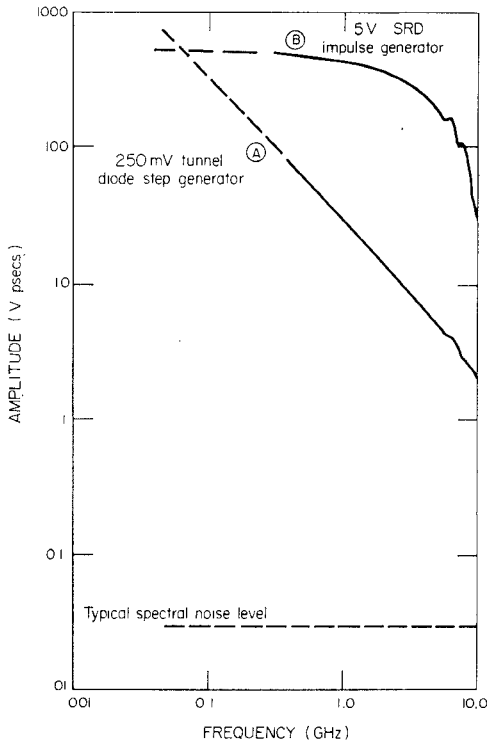

Fig. 3. Amplitude spectra of pulse generators.

ms. Such simple averaging, however, is only partially successful in reducing noise levels. This occurs because errors in the sampled value at a point are due to two main causes: a) additive noise voltages, which are contributed by oscilloscope amplifier circuits; and b) timing shifts, which occur because the precise triggering point of the oscilloscope timing ramp can vary slightly. The power spectra of both these errors can be obtained, and each shows a pronounced $1/f$ characteristic at real-time frequencies below about 1 Hz. This means that a measurement lasting several seconds or minutes cannot rely on simple averaging, which will not effect the very low-frequency drift components. To quote typical figures, with a 100-kHz generator and 1-ms time constant in the averaging circuit, short-term (>0.1 Hz) additive noise amounts to less than 1-mV rms, while over a long term (several minutes) the mean additive drift can amount to 10 mV or more. Similarly, short-term jitter amounts to about 2-ps rms, whereas long-term timing shifts can amount to more than 10 ps. The integral computer is used to sense these long-term drift components and compensate for them. This leaves the short-term components with a stationary mean value, and permits further averaging if required.

This compensation is achieved by causing the waveform to be scanned in a nonsequential fashion [6]. With reference to Fig. 4, a high-slope region of the overall scan window is selected, which must be outside the time window of interest if several waveforms have to be recorded within this window and compared. Points P_1,

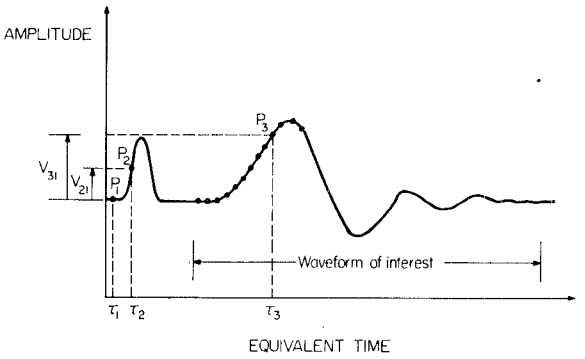

Fig. 4. Time-window stabilization.

P_2, and the initial position of P_3 within the time window are set manually, and then the computer automatically scans and computes the waveform slope around point P_2. In the computer configuration shown in Fig. 1, the digital quantity output-to-storage register R_1 represents the nominal horizontal position on the waveform at which the amplitude is to be measured. While scanning proceeds, the voltage difference V_{21} is repeatedly monitored and any changes are interpreted as horizontal timing shifts. The computer then derives a digital correction that is output-to-R_2 to cancel out this timing shift, restoring V_{21} to its original value. The computer stores successive values of V_{31}, which are now contaminated only by short-term noise and timing jitter.

When the effects of these two quasi-random-error sources are compared, an important conclusion emerges. If a waveform which rises 0.5 V in 50 ps is being measured, its maximum slope is 10 mV/ps. If short-term noise and jitter are 1-mV and 2-ps rms, respectively, then on the high-slope region of the waveform the total noise is approximately 20-mV rms, much higher than on regions of low slope. Since regions of high-slope frequently occupy only a few percent of the total time window, repeatedly scanning and averaging to reduce the noise variance at these few time positions is excessively time consuming. Accordingly, the computer is programmed to estimate the noise variance at each position, and continue averaging at that position until the variance of the mean of the readings is less than some present value. Another feature this offers is rejection of a set of readings if the variance is abnormally high, as occasionally happens due to a power-line transient. A single "rogue" point in time-domain data spreads its influence over the entire frequency domain after a Fourier transform is taken.

With the system which has been described, a typical measurement of 1024 points over a time window takes 4 to 5 min producing information over two frequency decades. In contrast, complex frequency-domain equipment is currently available which can, by electronically switching several octave-bandwidth swept-frequency sources, span a comparable total frequency range in a

few seconds. Although thus offering a comparatively slow measurement speed, time-to-frequency domain techniques do offer the following advantages over more conventional techniques.

1) Simplicity of instrumentation. The sampling system, computer and pulse generator are the three basic elements, and currently the cost of the minimum necessary computer approaches that of the oscilloscope.

2) Time windowing. The unique ability to carry out frequency analysis of only certain regions of the time-domain waveform allows the elimination of unwanted reflections and the deliberate positioning of multiple desired responses. This effect is exploited in the applications discussed below.

3) Simultaneous display of time- and frequency-domain responses. Frequently, useful information about the operation of a microwave network can be obtained from the juxtaposition of these two responses.

III. Applications to Networks and Materials Analysis

Time-to-frequency domain techniques have been applied to various broad-band microwave networks to obtain parameters conventionally measured by fixed or swept-frequency slotted line or bridge techniques [1]. The method is particularly suited to broad-band networks whose impulse response is comparatively short-lived, such as cables and attenuators, and unsuited (because of the excessive number of samples required) to narrow-band components with long transient responses. An example of a transmission measurement on a 4.1-GHz low-pass filter over 0.4 to 9.6 GHz is shown in Fig. 5 together with the waveforms from which it was derived. As an example of a reflection measurement, Fig. 6 shows the incident and reflected waveforms from a standard coaxial mismatch, together with the computed return loss.

The transient response to an incident impulsive wave of a thin slab of microwave material installed in a rigid coaxial line has been used [2] to yield the S_{11} and S_{21}^2 scattering parameters of the slab, and these in turn yield the complex permeability μ^* and permittivity ϵ^* of the material. In this work the experimental configuration shown in Fig. 2(d) was employed, where the "network under test" comprised the sample of material. A particular advantage of the arrangement is that the two independent measurements necessary in any system which measures μ^* and ϵ^* are obtained without displacing the sample. This then allows the sample to be in a stable extreme environment, such as at high temperature, while being measured.

This measurement illustrates the technique of providing a time reference point adjacent to a time window to stabilize the time frame when several waveforms must be measured within precisely the same window. Fig. 7 shows the measurement system, and open-circuit stubs S_T and S_R provide perturbations V_X and V_Y upon which time reference positions are established which

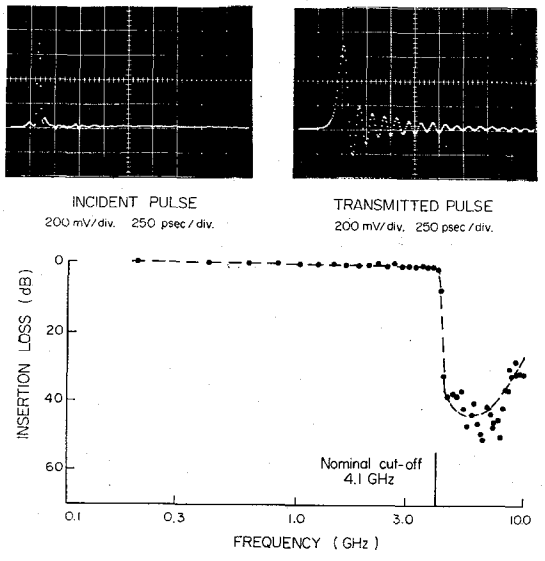

Fig. 5. Transmission amplitude of 4.1-GHz low-pass filter.

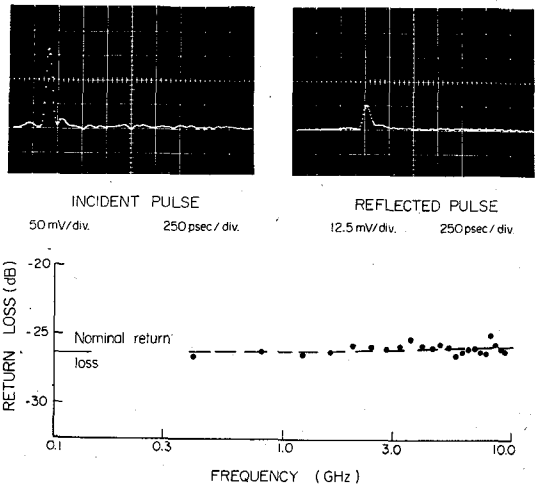

Fig. 6. Reflection amplitude of general radio WR110 standard mismatch.

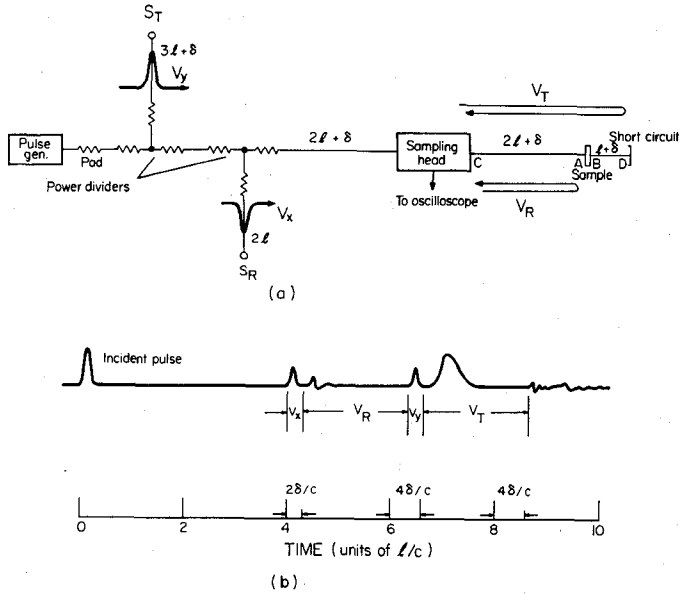

Fig. 7. Measurement of microwave materials. (a) Coaxial line system. (b) Sampling oscilloscope waveform.

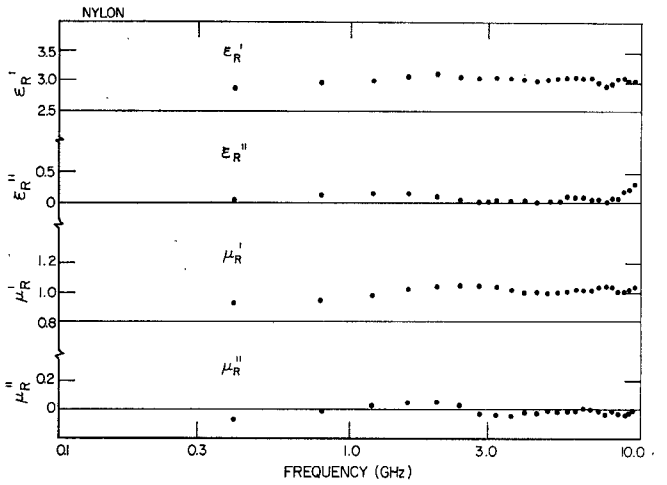

Fig. 8. Permittivity and permeability of Nylon.

stabilize the time windows V_R and V_T. Over time window V_R the reflected pulse from the sample of material is scanned and digitized, and over V_T the pulse transmitted twice through the sample is obtained. By replacing the sample of material by a metal slug and empty transmission line, respectively, inverted replicas of the incident pulse are obtained within V_R and V_T, respectively. These two sets of waveforms can be Fourier transformed to yield $S(\omega)$ and $S_{21}^2(\omega)$, and hence $\mu^*(\omega)$ and $\epsilon^*(\omega)$.

Typical results obtained by this technique for the constitutive parameters of a 0.25-in thick sample of Nylon in a 9/16-in diam coaxial line are shown in Fig. 8.

IV. Time-Domain Antenna Measurements

The properties of radiating structures can also be studied with time-domain techniques. Two useful measurements that can be made give frequency-domain parameters such as the receiving transfer function $H(\theta, \phi, \omega)$ and the driving-point admittance $Y_A(\omega)$ over a broad band of frequencies [7]. The methods used for these measurements are similar to those described above for microwave networks. In each case, the parameter is obtained for the entire bandwidth from one measurement.

Two parameters, $H(\theta, \phi, \omega)$ and $Y_A(\omega)$, can completely describe the circuit properties of an antenna. The receiving transfer function relates the voltage $V_L(\omega)$ measured across a load connected to the antenna terminals to a planar electric field $\vec{E}^i(\theta, \phi, \omega)$ incident on the antenna from some spatial angle θ, ϕ. It also represents the output of an equivalent circuit representation for the antenna. The generator voltage for this circuit is $\vec{h}_e(\theta,\phi,\omega)\cdot\vec{E}^i$, where $\vec{h}_e$ is the effective height. The generator admittance is $Y_A(\omega)$ and the load admittance is $Y_L(\omega)$. Thus,

$$V_L = HE^i = \frac{h_e E^i}{1 + Y_L/Y_A}.$$

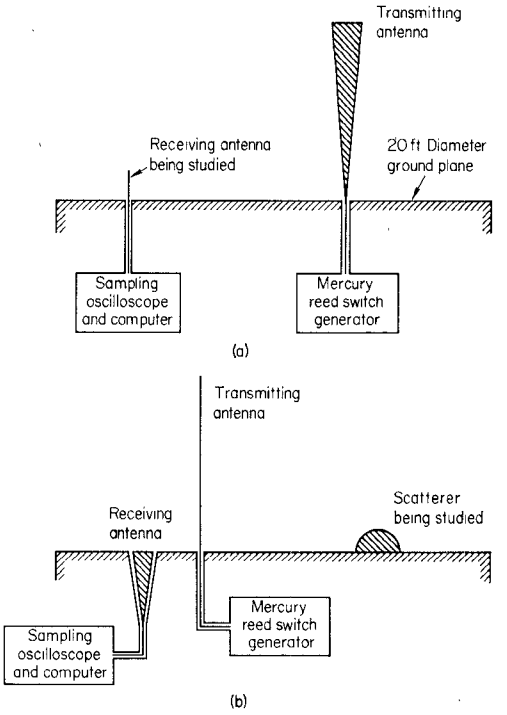

Fig. 9. Time-domain scattering range. (a) Antenna measurements. (b) Scattering measurements.

The transmission properties of the antenna can be calculated from the above parameters using the Rayleigh–Carson reciprocity theorem [8] relating the field factor $F_0(\theta, \phi, \omega)$ to the effective height, namely $F_0 = h_e \cdot \omega/c$.

Time-domain antenna measurements are performed on a large aluminum ground plane [9], as illustrated by Fig. 9(a). The ground plane isolates the measuring equipment from the space in which the measurements are performed. It is useful for studying antennas with a planar symmetry and an electrically balanced source or load. For most of the antenna studies, a long cone whose apex angle was very small ($\approx 2°$) was used as the transmitting antenna. Signals appear to radiate from the base or driving point of this antenna with no distortion relative to the generated voltage. Radiation also appears to emanate from the top of the cone. However, the position and length of the time window of observation are chosen so that this signal is incident on the receiving antenna after the end of the time window. The ground-plane range yields an interval of time after the arrival of the direct wave that is "uncontaminated" by unwanted reflections from the ground-plane edge and the walls of the room, thus eliminating the need for an anechoic chamber. A 300-V step waveform with a rise time less than 100 ps is applied to the terminals of the transmitting antenna.

There are two constraints on the receiving antenna being studied. The first is that the duration of its response for the incident signal used must be shorter than the time window. The second is that the antenna size must be small enough so that the spherical wavefront emanating from the base of the transmitting

antenna can be approximated by a plane wave for the shortest wavelengths in the spectrum of the incident signal (i.e., the Fraunhofer region) [10].

An example of the transmitted and received signal observed on the range is shown in Fig. 10(a) and (b). The receiving monopole had a height $h=8.7$ cm and a radius $a=0.31$ cm. The transfer function calculated by dividing the spectrum of the signal shown in Fig. 10(b) by that of Fig. 10(a) is shown in Fig. 10(c). The phase characteristic has been corrected for the propagation delay between generated and received signals. The accuracy, which appears to deteriorate significantly above 2.7 GHz, could have been extended by using more of the averaging processes discussed earlier.

Driving-point admittance measurements were made with the circuit shown in Fig. 2(b). The incident signal is observed as it first passes through the sampler, and the reflected signal is observed at a later time for the same measurement. The ratio of the spectra of the latter to the former gives the reflection coefficient. A bilinear transformation then yields the admittance. The measured admittance for the same monopole is shown in Fig. 11 in comparison with the theoretical values given by King [11] for an antenna with $\Omega=8$, where $\Omega=2$ ln $[(2h/a)]$. The agreement between the two sets of curves appears to be good for all of the frequencies for which data are available.

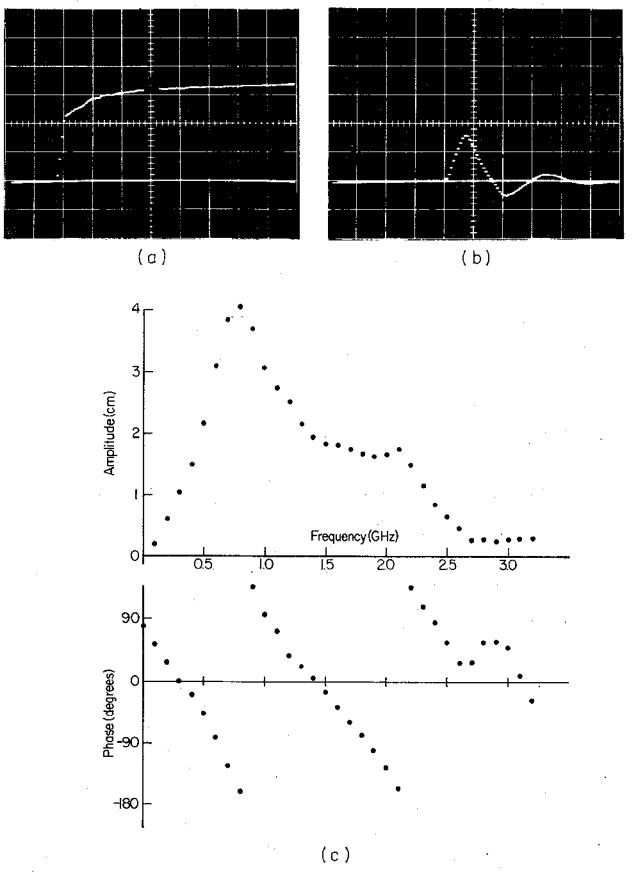

Fig. 10. Measured signals and transfer function for a monopole ($\Omega=8, h=8.7$ cm). (a) Transmitted step from long cone (1 ns/div). (b) Received signal (1 ns/div). (c) Measured transfer function (V/incident field).

V. Time-Domain Scattering Measurements

Scattering properties of bodies also have been obtained on the ground-plane range shown in Fig. 9(b). The response measured is the smoothed electromagnetic impulse response of the scattering bodies and contains useful frequency-domain information (both amplitude and phase) over a band that extends from 0.1 GHz up to about 4.5 GHz. Since this simple waveform contains frequency information over a wide band, it is a convenient characteristic signature of the target. Moreover, the smoothed impulse response is closely related to the actual target geometry and can provide useful insight into the actual scattering mechanism. From the smoothed impulse response the frequency response and the radar cross section can be obtained by application of the finite Fourier transform. Finally, since the smoothed impulse response contains both amplitude and phase information over a wide band, the response to any incident waveform whose spectrum lies within this band can be computed from it.

The transmit antenna for scattering measurements is a vertical monopole (long compared with the time interval of interest) and the receive antenna is a coaxial horn [12]. The receive antenna processes the radiated-step waveform to yield a smoothed impulse-voltage waveform at the output terminals. The radiated-step waveform also interacts with the target that has been placed on the ground plane, and the scattered wave reaches the receive antenna later in time. The voltage that appears at the output of the receive antenna due to the scattering by the target is the convolution of the

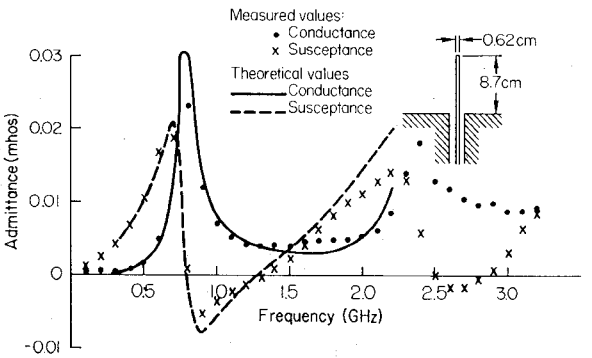

Fig. 11. Admittance of a monopole, $\Omega=8$.

target's impulse response with the output of the receive antenna due to the incident-step waveform. Thus, since the output due to the incident-step waveform is a smoothed impulse, this system measures the smoothed impulse response of the target directly.

In the actual measurement, the target is placed on the range and the scattered waveform is measured, digitized, and stored over the appropriate time window by the methods previously described. A second run over the same window may be taken with the target removed to permit subtraction of the residual baseline waveform which results from other small reflections on the range and the antennas. In these measurements the peak of

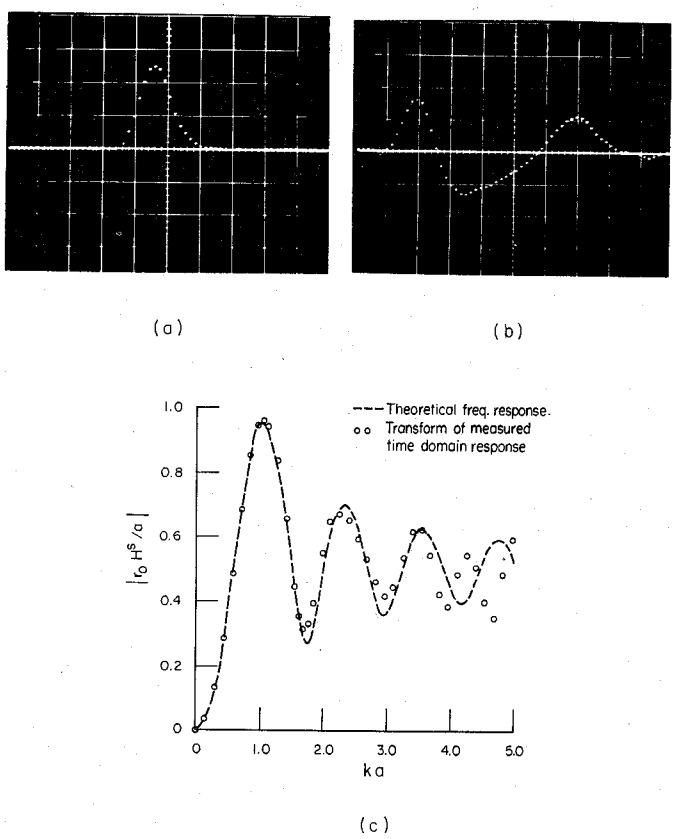

Fig. 12. Response of 4.25-in diam sphere. (a) Measured incident pulse (200 ps/div). (b) Measured sphere response (200 ps/div). (c) Frequency response of sphere (radius a).

the incident pulse, as measured on the sampling oscilloscope, is approximately 500 mV and a typical target response has a peak value in the vicinity of 10 mV. When using the 10-mV scale on the sampling oscilloscope, the estimated standard deviation in the sample mean of the voltage is less than 0.1 mV if 64 scans are averaged. Thus the standard deviation in the estimated voltage waveform is less than 1 percent of the peak value of the waveform.

The measured incident pulse is shown in Fig. 12(a), and the measured response of a 4.25-in diam sphere in the backscatter direction is shown in Fig. 12(b). The agreement between the measured response and the theoretical result obtained by solution of the space–time integral equation [13] is excellent [14]. The frequency response of a scattering body is computed from the measured incident pulse, and the resultant measured scattered response by using the finite Fourier transform approximation for the infinite Fourier transform, as described earlier. In Fig. 12(c) the frequency response obtained from the measured sphere data is compared with the theoretical frequency response of the sphere calculated with classical techniques. The agreement is good up to a ka of approximately 4. This range of good agreement is limited primarily by the spectral content of the incident pulse and could be extended by using larger targets and/or shorter pulses. Numerous other measurements of scattering properties can be performed for bodies which include right-circular cylinders, right-square cylinders, sphere-capped cylinders, cores, cubes, and others [3], [15], [16].

VI. Conclusion

This paper illustrates the broad range of application of time-domain techniques to common microwave measurements. While limited by the spectral intensities available from current subnanosecond pulse generators to acquisition times for a complete waveform amounting to several minutes, the very broad bandwidth available from the transformed response can in fact represent a savings in setup time relative to conventional point-by-point measurements. With the development of new forms of solid-state pulse generators and sampling techniques, it is expected that even more applications will appear for microwave time-domain metrology.

Acknowledgment

The authors wish to thank Dr. G. F. Ross for his leadership and guidance in initiating and encouraging this research in the new field of time-domain electromagnetics; Dr. J. D. DeLorenzo for his many valuable contributions—in particular those which brought the time-domain measurement range to its practical realization; and R. S. Smith for his major contribution to the software required to bring the measurement techniques to their current status.

References

[1] A. M. Nicolson, "Broad-band microwave transmission characteristics from a single measurement of the transient response," *IEEE Trans. Instrum. Meas.*, vol. IM-17, pp. 395–402, Dec. 1968.
[2] A. M. Nicolson and G. F. Ross, "Measurement of the intrinsic properties of materials by time-domain techniques," *IEEE Trans. Instrum. Meas.*, vol. IM-19, pp. 377–382, Nov. 1970.
[3] G. F. Ross *et al.*, "A time domain electromagnetics bibliography," Sperry Rand Res. Ctr. Res. Rep. RR-70-30, Feb. 1971.
[4] G. D. Bergland, "A guided tour of the fast Fourier transform," *IEEE Spectrum*, vol. 6, pp. 41–52, July 1969.
[5] B. J. Elliott, "Picosecond pulse measurements of the conduction current versus voltage characteristics of semiconductor materials with bulk negative differential conductivity," *IEEE Trans. Instrum. Meas.*, vol. IM-17, pp. 330–332, Dec. 1968.
[6] A. M. Nicolson, "Wideband system function analyzer employing time to frequency domain translation," WESCON Conv., Session 22, San Francisco, Aug. 1969.
[7] L. Susman and D. Lamensdorf, "Picosecond pulse antenna techniques," Final Tech. Rep. RADC-TDR-71-64, under Contract F33615-70-C-0088, May 1971.
[8] H. J. Schmitt, "Transients in cylindrical antennae," Monogr. 377E, pp. 292–298, Apr. 1960.
[9] J. D. DeLorenzo, "A Range for measuring the impulse response of scattering objects," NEREM, Nov. 1967.
[10] J. D. Kraus, *Antennas*. New York: McGraw-Hill, 1950, p. 6.
[11] R. W. P. King, *Theory of Linear Antennas*. Cambridge, Mass: Harvard Univ. Press, 1956, p. 170.
[12] D. Lamensdorf, "The transient response of the coaxial cone antenna," presented at the 1969 Int. Antenna and Propagation Symp., Austin, Tex., Dec. 1969.
[13] C. L. Bennett, "A technique for computing approximate electromagnetic impulse response of conducting bodies," Ph.D. dissertation, School of Electrical Engineering, Purdue Univ., Lafayette, Ind., Aug. 1968.
[14] C. L. Bennett and J. D. DeLorenzo, "Short pulse response of radar targets," presented at the 1969 Int. Antenna and Propagation Symp., Austin, Tex., Dec. 1969.
[15] R. S. Smith *et al.*, "Wideband surface current analysis," Final Tech. Rep. RADC-TR-70-188, under Contract F30602-69-C-0357, Nov. 1970.
[16] C. L. Bennett *et al.*, "Integral equation approach to inverse scattering," Final Tech. Rep. RADC-TR-70-177, under Contract F30602-69-C-0332, Oct. 1970.